ISSN 1870-4069

Utility-Pole, Nuts and Cross-Arm Visual Detection, for Electric Connections Maintenance Robot

José Luis Gómez Torres[1], Saúl Martínez Díaz[1], Iris Iddaly Méndez Gurrola[2], Alejandro Israel Barranco Gutiérrez[3], Kyoichi Tatsuno[4]

[1] TecNM La Paz,
Mexico

[2] Universidad Autónoma de Ciudad Juárez,
Mexico

[3] Cátedras CONACyT-TecNM Celaya,
Mexico

[4] Meijo University, Nagoya,
Japan

israel.barranco@itcelaya.edu.mx

Abstract. In this work, a computer vision system used by a utility-pole maintenance robot is presented. The objective of the system is that the robot repairs connections between cables and screws on the utility-pole. To accomplish this task, it uses a pair of cameras that detects and locates the utility pole, crosstree, nuts, and screws. The detection is based on color, shape and dimensions analysis, by using conventional RGB cameras. On the other hand, the challenges facing this approach include: utility-pole detection though in the same scene, some objects with the same color (concrete) appear; flexibility in the distance between cameras and utility-pole for detection and localization, about 2-10 meters range and slope estimation of utility-pole and crosstree. The experiments show that it is possible to recognize and locate the interest pieces with satisfactory results and they encourage to expand the current system capabilities.

Keywords: Utility Pole, Maintenance Robot, Object Recognition, Object Location.

1 Introduction

In the last fifty years, developments in robotics have grown exponentially (Cianchetti, 2014), thus these systems are used to improve the life quality of humans in different environments.

In this context, a maintenance robot who repair cable connections on utility-poles (UPs) is been constructed at Tatsuno Laboratory at Meijo University to avoid the risk when electric technicians make this work. As a human, an android needs to recognize the UP, cables, screws, nuts, thus dimensions and locations (Y. He, 2008), (Barranco-Gutierrez, Martínez Díaz, & Gomes Torres, An Approach for Utility Pole Recognition in Real Conditions, 2014) to execute this task. Due to the grown-on algorithms development for processing digital images, it estimated possible that their techniques could perform the mentioned tasks.

In literature, there are many techniques for object recognition, but with the searching it was observed that there are few object recognition techniques outdoors and practically nil in recognizing UP. Concerning to objects location in 3D coordinates, it observed that exist many probabilistic algorithms, but they have different restrictions; so, the use of stereo vision system was selected because it has fewer restrictions to calculate positions in 3D than monocular systems, some experiments were performed using this technique (Barranco-Gutierrez, Martínez Díaz, & Gomes Torres, An Approach for Utility Pole Recognition in Real Conditions, 2014).

This work used Mexican UPs to experiment in thus detection algorithms under solar lighting. The system detects the UP in the range of 15 to 3 meters from camera to the target. This paper shows improvement to the system for example: it works with a Japanese element UP, the crosstree, screws, nuts and the holes (where the screws are inserted) are detected and located. This, using only one set of color stereoscopic vision. In Fig. 1 is shown the prototype of this research.

1.1 Related Work

Although there are many object recognition techniques. There are few concrete proposals to solve the problem of the recognition of Electric Poles due to the specificity of the problem and the challenges involved in solving it. For example, the large number of pole-like objects on the street such as PVC pipes, telephone poles, traffic signs, and cable TV poles. In (Zhang, et al., 2018), the authors proposed using a deep learning-based method for automatically mapping roadside utility poles with crossarms (UPCs) from Google Street View (GSV) images.

The method combines the state-of-the-art DL object detection algorithm (i.e., the RetinaNet object detection algorithm) and a modified brute-force-based line-of-bearing (LOB, a LOB stands for the ray towards the location of the target [UPC at here] from the original location of the sensor [GSV mobile platform]) measurement method to estimate the locations of detected roadside UPCs from GSV. Also, in (Watanabe, 2018) a deep network is used to detect utility poles. The authors found that the electric poles can be detected with an average precision (AP) of 72.2%. Their results demonstrate the operational feasibility of the autonomous electric pole inspection system that implements a deep network-based object detector.

Reference (Y. He, 2008) proposes an approach for automatically inputting handwritten Distribution Facility Drawings (DFD) and their maps into a computer, by using the Facility Management Database (FMD).

The recognition method makes use of external information for drawing/map recognition. It identifies each electric-pole symbol and supports cable symbol on drawings simply by consulting the FMD, but the system requests manual feedback from

the operator in online stage. Reference (Barranco-Gutierrez, Martínez Díaz, & Gomes Torres, An Approach for Utility Pole Recognition in Real Conditions, 2014) presents an algorithm for the recognition of similar electrical poles from an aerial image by detecting the pole shadow. One pole is used as a template (already identified by a human operator) for the algorithm.

Fig. 1. Prototype in Tatsuno Laboratory illustrates the UP, manipulator robot and stereo vision system.

The algorithm includes feature extraction, utility pole position determination and elimination of redundant candidates. This work references the ideas from other works in a similar sense, the papers (Nakajima, 1995) (Cetin, 2009) detail, although the color distribution changes under different lighting conditions, some aspects of its structure turn out to be invariants. In the works (Igor, Amit, & Ehud, 2013) (Berwick & Lee, 1998), it explains that the sky has always been the crucial element in modeling the

background of an outdoor scene. The position of the sun during the day gives a different impact on the sky color. The method presented in (Halawani & Sunar, 2010) is used to compare our method although the acquisition system is different. In other outdoor computer vision applications such as autonomous vehicles. It also presents the challenges of lighting from the sun, the large number of different objects, shadows, reflections, occlusions and the high similarity between some objects (Janai, Güney, Behl, & Geiger, 2020).

2 Proposed Methodology

The training and on-line checking stages use a very similar methodology; the unique difference in the training stage, it consists in the possibility to monitor the results and modify some constants values for tuning the system according to the problem conditions. The procedure is based on three basic aspects of computer vision: Color, shape and dimensions. This is, the implemented techniques are: thresholding on HSV scheme to filter by color, Hu invariants to describe shapes and stereo vision to measure objects dimensions. All of them, combined to detect and locate utility-poles with its crosstree, nuts and screws. Below, the approach steps to detect the utility-pole, are listed:

I. Stereo image acquisition,
II. HSV conversion,
III. Color thresholding,
IV. Canny edge detector,
V. Lines detector,
VI. AND operation,
VII. Hu invariants, slope and area calculus,
VIII. Classification stage,
IX. Stereo matching and utility pole localization.

I. Stereo Image Acquisition

To take photographs in the stereo vision system, it must be calibrated (Barranco-Gutierrez, Martínez-Díaz, & Gomez-Torres, Visión estereoscópica con Matlab y OpenCV, 2018). This means that it must to know, the vector between both camera reference technically, to have the fundamental and essential matrices of stereoscopic system as indicate (Zisserman & Hartley, 2003), (Zhang Z. , 2000). After this, we can start training or on-line work. In the image acquisition system, a color image is received from the left and right cameras with resolution $M\ x\ N\ x\ 3$ (M for rows, N for columns and three-color components) with $b = 10$ bits of resolution for each pixel and the stereo image is expressed in both sides $I^s = I^{\text{left}}$ or $I^s = I^{right}$ in equations in equation (1):

$$I^s(x, y, z) \in \{0 \leq \mathbb{Z} \leq 2^b\}, \tag{1}$$

where x, y, z are indexes that locate to each pixel and $\mathbb{Z}$ is the set of integer numbers. $z = 0$ refers to the image's RED component, $z = 1$ the image's GREEN component and $z = 2$ the image's BLUE component.

II. HSV Conversion

In this step, the program converts the left and right images to HSV space as indicates by equations (2, 3, 4) in order to obtain a color information in the axis H:

$$H(x,y) = \begin{cases} undefined \quad if \quad \max(R,G,B) = min(R,G,B), \\ \dfrac{\pi(G-B)}{3(\max(R,G,B) - \min(R,G,B))} \quad if \quad \max(R,G,B) = R \quad and \quad G \geq B, \\ \dfrac{\pi(G-B)}{3(\max(R,G,B) - \min(R,G,B))} + 2\pi \quad if \quad \max(R,G,B) = R \quad and \quad G < B, \\ \dfrac{\pi(G-B)}{3(\max(R,G,B) - \min(R,G,B))} + \dfrac{2\pi}{3} \quad if \quad \max(R,G,B) = G, \\ \dfrac{\pi(G-B)}{3(\max(R,G,B) - \min(R,G,B))} + \dfrac{4\pi}{3} \quad if \quad \max(R,G,B) = B, \end{cases} \tag{2}$$

$$S(x,y) = \begin{cases} 0 \quad if \quad \max(R,G,B) = 0, \\ 1 - \dfrac{\min(R,G,B)}{\max(R,G,B)} \quad if \quad \max(R,G,B) \neq 0, \end{cases} \tag{3}$$

$$V(x,y) = \max(R,G,B), \tag{4}$$

where $R^s(x,y) = I^s(x,y,1)$, $G^s(x,y) = I^s(x,y,2)$, $B^s(x,y) = I^s(x,y,3)$, the function $max(R,G,B)$ retrieves the maximum value among its three arguments and in contrast, $min(R,G,B)$ obtains the minimal.

III. Color Thresholding

Because the H component of the RGB conversion to HSV contains the color information of objects in the image and component V describes the lighting in qualitative terms, a filter with the desired color and lighting is constructed using a range within a Gaussian distribution function as described in (5):

$$BW^s(x,y) = \begin{cases} 1 \quad if\ H^s(x,y) < \mu_h\ AND\ S^s(x,y) < \mu_s\ \ AND\ \ V^s(x,y) < \mu_v\ , \\ 0 \quad otherwise. \end{cases} \tag{5}$$

IV. Canny Edge Detector

To find contours from the thresholded $BW^s(x,y)$, the Canny method is used, in order to delimit objects with the same color, (6):

$$C^s(x,y) = Canny\big(BW^s(x,y)\big). \tag{6}$$

V. Lines Detector

Then, in the resulting images, lines between 80 and 100 degrees are detected using Hough transform from the edge image, in order to delimit the utility pole, (7):

$$Ho^s(x,y) = Hough\big(BW^s(x,y), \mu_{Hough(s)}\big). \tag{7}$$

VI. AND Operation

In order to get a reliability edges, a combination of $C(x,y)$ and $Ho(x,y)$ is calculated, (8):

$$E^s(x,y) = C^s(x,y)\ AND\ \text{Hough}\big(BW^s(\text{x},\text{y}), \mu_{Hough(s)}\big). \tag{8}$$

Because it describes each edge in the image, the process of connected components labeling runs using the iterative method, (9):

$$L_i^s(x,y) = labeling\big(E^s(x,y)\big), \tag{9}$$

where $O_i \cap O_j \in \emptyset \quad \forall\ j \neq i$ for all $i,j = 1,2,3 \dots, LN$.

VII. Hu Invariants, Slope and Area Calculus

Each labeled edge is described using the seven Hu invariants, (10):

$$[\phi_{1,i}^s, \phi_{2,i}^s, \phi_{3,i}^s, \phi_{4,i}^s, \phi_{5,i}^s, \phi_{6,i}^s, \phi_{7,i}^s]) = Hu(L_i^s(x,y)). \tag{10}$$

VIII. Classification Stage

In this work, the classification stage is implemented with 10 neurons in hidden layer Neural Network (NN), trained to identify the shape of utility-pole using Hu invariants equation (11). Its architecture consists in fourteen inputs connected to a "tansig" neuron and a "logsig" function at the output:

$$O_i^s = NN\big(\phi_{1,i}^s, \phi_{2,i}^s, \phi_{3,i}^s, \phi_{4,i}^s, \phi_{5,i}^s, \phi_{6,i}^s, \phi_{7,i}^s\big), \tag{11}$$

where O_i^s has binary values, 0 to indicate that is not a utility pole and 1 to express that is a utility pole edge.

X. Stereo Matching and Utility Pole Localization

The centroid of $L_k^s(x,y)$ for $O_i^s = 1$, is calculated in order estimate the location of utility-pole for $s = left$ and $s = right$ using equation (12):

$$(C_x^s, C_x^s) = centroid\big(L_k^s(x,y)\big). \tag{12}$$

Finally, the location of the utility-pole is triangulated using the characteristics of the stereo vision system, (13):

$$\big(P_x, P_y, P_z\big) = triangulation\big(C_x^{left}, C_y^{left}, C_x^{right}, C_y^{right}\big). \tag{13}$$

Once the pole has been detected, next step is the detection of the crosstree and to estimate the position of the screws and nuts. To achieve this firstly the holes in the crosstree are detected, and from these, the 3D position of the nuts is calculated. The steps for this are listed below:

a. Detection of horizontal lines.

b. Region of interest (ROI) creation including the cross-arm.

c. Thresholding of the ROI.

d. Holes detection by circularity.

e. Holes matching based on the fundamental matrix.

f. Triangulation of the position of each hole is based on two images.

g. Line fitting of the triangulated holes.

h. Estimation of the nuts position.

To perform the holes matching the following property of the stereo systems is used:

$$p'Fp = 0, \tag{14}$$

where *F* is the Fundamental Matrix of the stereo system and *p* is a 3D point in the scene captured by the cameras.

3 Experiments

The experiment was developed in the Tatsuno laboratory under controlled lighting, i.e., lighting with conventional lamps. The cameras used are Sony EVI-D70 with resolution 768 x 494 pixels. The system was tested with Japanese harnesses and utility-pole. After acquiring both stereoscopic pictures of system, we proceed to conversion from RGB to HSV and the result is shown in Fig. 2, to filter by color. In this case, using the ranges defined in Table 1.

Table 1. Color range for the interest objects (Utility-poles).

	Min	Max
Left Image Hue	54	198
Left Image Saturation	7	86
Left Image Value	20	64
Right Image Hue	23	213
Right Image Saturation	9	75
Right Image Value	20	66

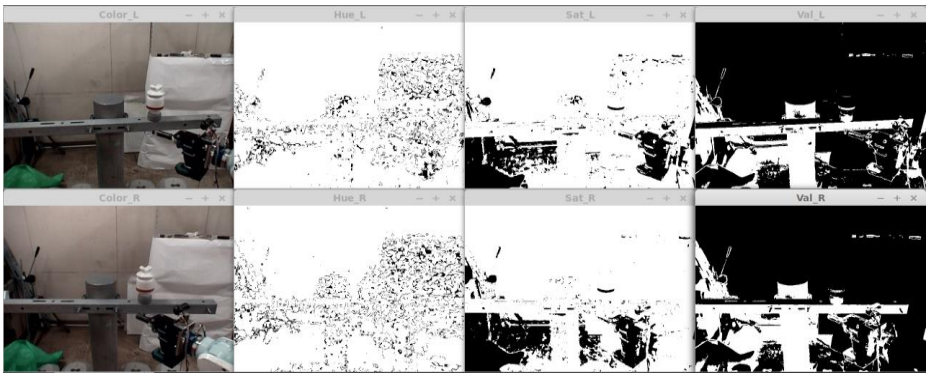

Fig. 2. Stereo image acquisition and RGB to HSV conversion.

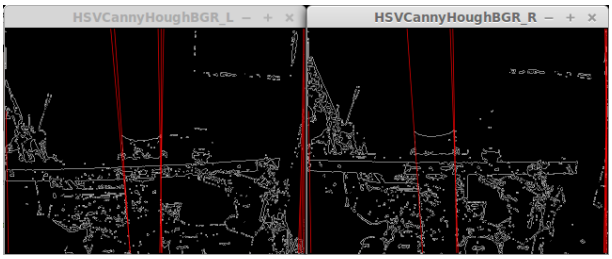

Fig. 3. Lines detected in a range of 80 to 100 degrees.

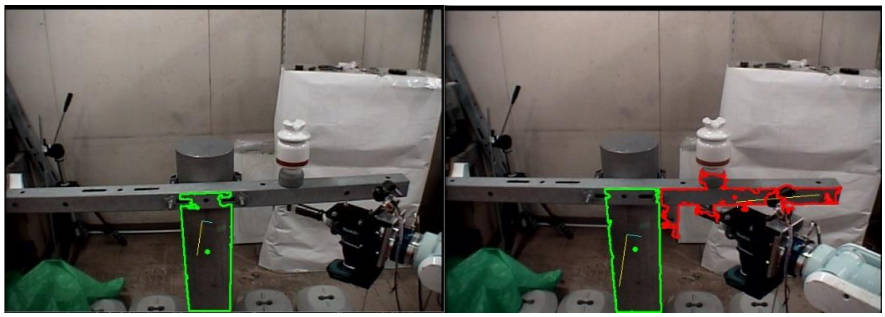

Fig. 4. Utility pole segment detected by using color, shape and dimensions.

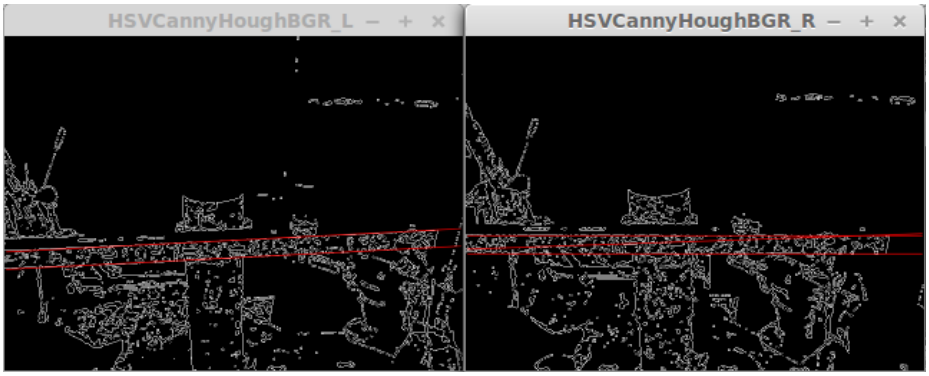

Fig. 5. Lines detected in a range of -10 to 10 degrees.

Fig. 6. Cross-arm detected and segmented.

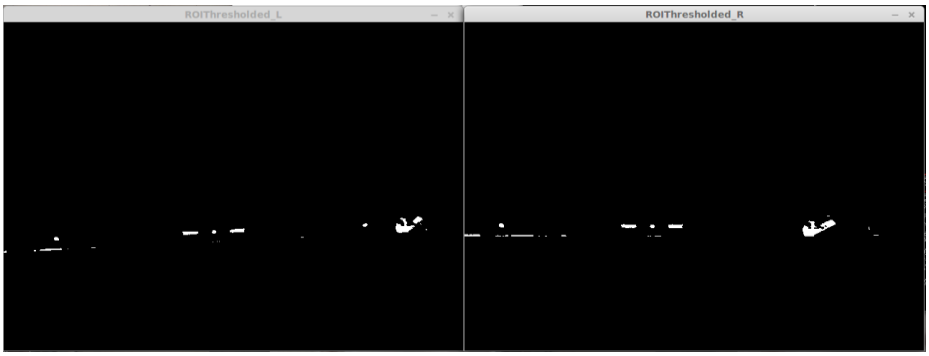

Fig. 7. Cross-arm ROI, binarized and complemented.

The next stage (IV is to find contours in the thresholded (BW) images, using the Canny method for it. Then, in the resulting images, approximately vertical lines are detected (V stage), between 80 and 100 degrees. This aims to separate the pole and background objects that have approximately the same color, which would alter the shape of the blob detected, affecting the invariants calculation.

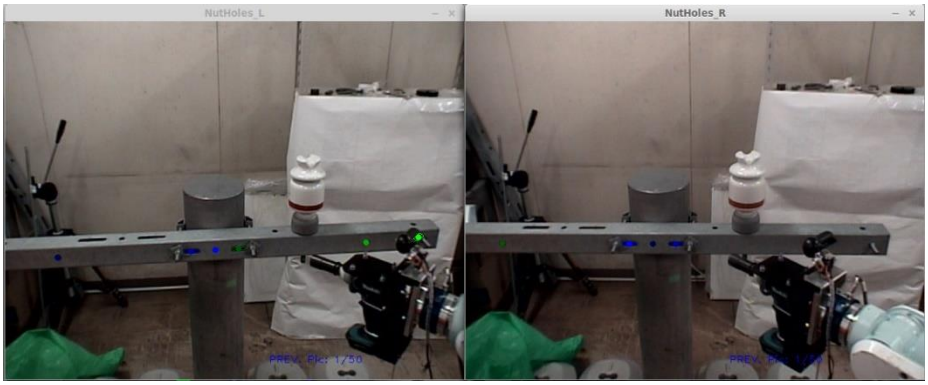

Fig. 8. Detected holes.

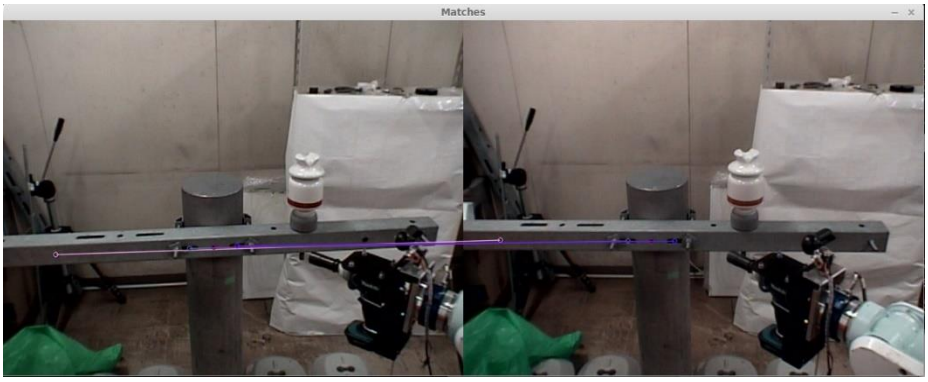

Fig. 9. Matched Holes.

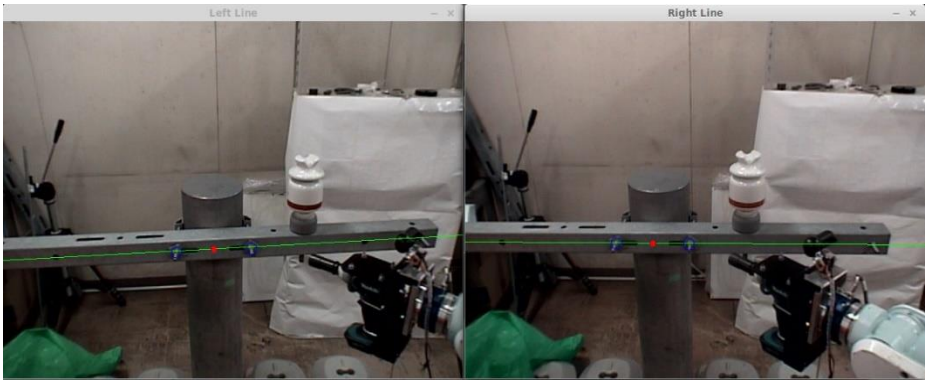

Fig. 10. Located nuts.

The selection of the threshold for the lines detection by Hough method is an important issue because if a very high threshold is selected only one side of the pole could be detected, whereas with a very low threshold, many lines are detected and if

some of these lines cross the pole also affects the detection process. In this case, 72 and 71 values have been selected for the left and right cameras, respectively. In Fig. 3, it can be seen the lines detected with these thresholds.

Once the vertical lines are found, there are negated and AND operated with the color thresholded images in order to separate the pole from the background (VI stage). At this point we have the blobs in the image which correspond to the interest objects; for every blob, Hu invariants, slope and area are calculated in order to classify the blob (VIII stage).

Note: A prior training run is required for the Neural Network (NN) to be able to properly classify. Objects classified as utility-poles are highlighted in green, objects classified as not pole are highlighted in red, as shown in Fig. 4. If the NN is unable to accurately classify the object, it is highlighted in blue.

After this stage the pole has been found in both images (in case it appears at the cameras view) and a triangulation is performed using the pole centroid in both images to spatially locate it, relative to the left camera (stage IX).

Once the pole has been detected, next step is the detection of the crosstree and to estimate the position of the screws and nuts. To achieve this firstly the holes in the crosstree are detected, and from these, the 3D position of the nuts is calculated. The Fig. 5 shows the (a) step.

After the lines are detected a ROI is created with them, as shown in Fig. 6. The Fig. 7 and 8 show the result of the (c) and (d) steps.

To perform the holes matching the stereo epipolar property equation (14) is used. Instead of 0 a sufficient small ϵ value is adopted.

This value change with the stereo calibration. So, values between 0.05 and 0.15 are recommended to start.

After this step the holes have been detected and matched in both images, whereby the position of each of them can be triangulated and proceed to step g. It makes a 3D line fitting with all hole points; finding this line and knowing the physical distance from the center hole of the cross-arm to the nuts, the position of these can be calculated, as shown in Fig. 9.

Finally, the 3D position of the last point is found, in this case, the upper right corner of the front face of the crossarm, and thus the plane thereof is calculated, with this, the normal vector to that plane is obtained, i.e., the direction of the screws.

Therefore, although the system supports changes in perspective, must be ensured that both cameras can watch the right corner of the front face of the cross-arm to calculate the orientation of the screws as illustrates Fig. 10.

4 Discussion

This work is an extension of that developed in reference (Barranco-Gutierrez, Martínez Díaz, & Gomes Torres, An Approach for Utility Pole Recognition in Real Conditions, 2014). Table 2 shows the main differences, which include crosstree and nuts detection and localization. The last stage has not been tested outdoor yet; however, pole detection was successfully tested before, in extreme illumination conditions.

The neural network was trained with 50 images from each camera. In each training image one segmented object from the true class (UP) and one segmented object from

Table 2. Methods comparison.

Feature	Barranco et al. 2014	Actual proposal
Utility-pole detection	Yes	Yes
Under Solar illumination	Yes	Not
Cross-arm detection and location	Not	Yes
Nuts detection and location	Not	Yes
Japanese UP detection and location	Not	Yes
Mexican UP detection and location	Yes	Yes

Table 3. Confusion matrix.

Output/target	UP	Non-UP
UP	40%	0%
Non-UP	10%	50%

Table 4. Proposals comparison.

	(Zhang, et al., 2018)	(Watanabe, 2018)	Actual proposal
Average precision	79%	72%	90%

the false class (non-UP) were selected. The training error reached a value below 1%. The whole system was tested in real time with 25 non-training images from each camera. The system tried to select the UPs among all the segmented objects into each processed image.

Table 3 shows the confusion matrix resulting from the test where the percentage of true positives is 40%, true negatives 0%, false positives 10% and false negatives 50%. Note that, in some cases, the system was unable to detect the UP due to a bad segmentation of the image.

However, once detected the UP, the system detected the cross arm and the nuts 100% of the time. In Table 4 is shown the comparison between some actual proposals on this topic.

5 Conclusions

The proposed computer vision system designed to detect Japanese utility-poles and its nuts and crosstree, identifies correctly the aims in ninety percent. Which means it has a good performance under the conditions that have it now. Although neural networks have shown great ability to classify nonlinear problems, the HSV color model

description and the shape characterization of Hu invariants, greatly helped to obtain the results shown in the work. Regarding the measurement of the dimensions of objects in the 3D environment, stereoscopic configuration helps to facilitate the calculations of depth and longitudinal dimensionality of objects. So, it has a classification by color, shape and dimensions of interest objects. Cables and ceramic insulator type bell detection is the next stage to accomplish for the robotic maintenance task. To work again under solar lighting conditions and test the entire system in real conditions.

Acknowledgments. The authors greatly appreciate the support of PROMEP and CONACyT with the project 215435. Also, we want to thanks to Cesar Cerezo by his valuable support to construct this work.

References

1. Barranco-Gutierrez, A.I., Martínez-Díaz, S., Gomes-Torres, J.L.: An approach for utility pole recognition in real conditions. Lecture Notes in Computer Science, pp. 113−121, Springer (2014)
2. Barranco-Gutierrez, A.I., Martínez-Díaz, S., Gomez-Torres, J.L.: Visión estereoscópica con Matlab y OpenCV. Pearson (2018)
3. Berwick, D., Lee, S.: A chromaticity space for specularity, illumination color and illumi-nation pose-invariant 3-D object recognition. International Conference on Computer Vision, pp. 165−170 (1998)
4. Cetin, B.: Automated electric utility pole detection from aerial images. SOUTHEASTCON'09, pp. 44−49 (2009)
5. Cianchetti, C.L.: Soft robotics: new perspectives for robot bodyware and control. Frontiers in Bioengineering and Biotechnology, 1 (2014)
6. Halawani, S.M., Sunar, M.S.: Interaction between sunlight and the sky colour with 3D objects in the outdoor virtual environment. Fourth Asia International Conference on Mathematical/Analytical Modelling and Computer Simulation, pp. 470−475, IEEE Computer society (2010)
7. Igor, K., Amit, A., Ehud, R.: Color invariants for person reidentification. IEEE Transactions on Pattern Analysis and Machine Intelligence, pp. 1622−1634 (2013)
8. Janai, J., Güney, F., Behl, A., Geiger, A.: Computer vision for autonomous vehicles: problems, datasets and state of the art. Foundations and Trends® in Computer Graphics and Vision, pp. 1−308 (2020)
9. Nakajima, C.: Automatic recognition of facility drawings and street maps utilizing the facility management database. Third International Conference on Document Analysis and Recognition, pp. 516−519 (1995)
10. Watanabe, J.I.: Electric pole detection using deep network based object detector. SPIE Remote Sensing, SPIE (2018)
11. He, K.T.: An example of open robot controller architecture for power distribution line maintenance robot system. World Academy of Science, Engineering and Technology, pp. 266−271 (2008)
12. Zhang, W., Witharana, C., Li, W., Zhang, C., Li, X., Parent, J.: Using deep learning to identify utility poles with crossarms and estimate their locations from google street view images. Sensors, pp. 1−21 (2018)

13. Zhang, Z.: Flexible new technique for camera calibration. IEEE Transactions on Pattern Analysis and Machine Intelligence, pp. 1330−1334 (2000)
14. Zisserman, A., Hartley, R.: Multiple view geometry in computer vision. Cambridge University Press (2003)